

Evidence from d+Au measurements for final-state suppression of high p_T hadrons in Au+Au collisions at RHIC

J. Adams,³ C. Adler,¹² Z. Ahammed,²⁵ J. Amonett,¹⁵ B.D. Anderson,¹⁵ M. Anderson,⁵ D. Arkhipkin,¹¹ G.S. Averichev,¹⁰ J. Balewski,¹³ O. Barannikova,^{25,10} L.S. Barnby,¹⁵ J. Baudot,¹⁴ S. Bekele,²² V.V. Belaga,¹⁰ R. Bellwied,³⁶ J. Berger,¹² B.I. Bezverkhny,³⁸ H. Bichsel,³⁵ A. Billmeier,³⁶ L.C. Bland,² C.O. Blyth,³ B.E. Bonner,²⁶ M. Botje,²¹ A. Boucham,³⁰ A. Brandin,¹⁹ A. Bravar,² R.V. Cadman,¹ X.Z. Cai,²⁹ H. Caines,³⁸ M. Calderón de la Barca Sánchez,² A. Cardenas,²⁵ J. Carroll,¹⁶ J. Castillo,¹⁶ M. Castro,³⁶ D. Cebra,⁵ P. Chaloupka,⁹ S. Chattopadhyay,³⁶ H.F. Chen,²⁸ Y. Chen,⁶ S.P. Chernenko,¹⁰ M. Cherney,⁸ A. Chikanian,³⁸ B. Choi,³² W. Christie,² J.P. Coffin,¹⁴ T.M. Cormier,³⁶ J.G. Cramer,³⁵ H.J. Crawford,⁴ A.A. Derevschikov,²⁴ L. Didenko,² T. Dietel,¹² X. Dong,^{28,16} J.E. Draper,⁵ F. Du,³⁸ V.B. Dunin,¹⁰ J.C. Dunlop,² V. Eckardt,¹⁷ L.G. Efimov,¹⁰ V. Emelianov,¹⁹ J. Engelage,⁴ G. Eppley,²⁶ B. Erazmus,³⁰ P. Fachini,² V. Faine,² J. Faivre,¹⁴ R. Fatemi,¹³ K. Filimonov,¹⁶ P. Filip,⁹ E. Finch,³⁸ Y. Fisyak,² D. Flierl,¹² K.J. Foley,² J. Fu,^{16,37} C.A. Gagliardi,³¹ T.D. Gutierrez,⁵ N. Gagunashvili,¹⁰ J. Gans,³⁸ L. Gaudichet,³⁰ M. Germain,¹⁴ F. Geurts,²⁶ V. Ghazikhanian,⁶ J.E. Gonzalez,⁶ O. Grachov,³⁶ V. Grigoriev,¹⁹ D. Grosnick,³³ M. Guedon,¹⁴ S.M. Guertin,⁶ E. Gushin,¹⁹ T.J. Hallman,² D. Hardtke,¹⁶ J.W. Harris,³⁸ M. Heinz,³⁸ T.W. Henry,³¹ S. Heppelmann,²³ T. Herston,²⁵ B. Hippolyte,³⁸ A. Hirsch,²⁵ E. Hjort,¹⁶ G.W. Hoffmann,³² M. Horsley,³⁸ H.Z. Huang,⁶ S.L. Huang,²⁸ T.J. Humanic,²² G. Igo,⁶ A. Ishihara,³² P. Jacobs,¹⁶ W.W. Jacobs,¹³ M. Janik,³⁴ I. Johnson,¹⁶ P.G. Jones,³ E.G. Judd,⁴ S. Kabana,³⁸ M. Kaneta,¹⁶ M. Kaplan,⁷ D. Keane,¹⁵ J. Kiryluk,⁶ A. Kisiel,³⁴ J. Klay,¹⁶ S.R. Klein,¹⁶ A. Klyachko,¹³ D.D. Koetke,³³ T. Kollegger,¹² A.S. Konstantinov,²⁴ M. Kopytine,¹⁵ L. Kotchenda,¹⁹ A.D. Kovalenko,¹⁰ M. Kramer,²⁰ P. Kravtsov,¹⁹ K. Krueger,¹ C. Kuhn,¹⁴ A.I. Kulikov,¹⁰ G.J. Kunde,³⁸ C.L. Kunz,⁷ R.Kh. Kutuev,¹¹ A.A. Kuznetsov,¹⁰ M.A.C. Lamont,³ J.M. Landgraf,² S. Lange,¹² C.P. Lansdell,³² B. Lasiuk,³⁸ F. Laue,² J. Lauret,² A. Lebedev,² R. Lednický,¹⁰ V.M. Leontiev,²⁴ M.J. LeVine,² C. Li,²⁸ Q. Li,³⁶ S.J. Lindenbaum,²⁰ M.A. Lisa,²² F. Liu,³⁷ L. Liu,³⁷ Z. Liu,³⁷ Q.J. Liu,³⁵ T. Ljubicic,² W.J. Llope,²⁶ H. Long,⁶ R.S. Longacre,² M. Lopez-Noriega,²² W.A. Love,² T. Ludlam,² D. Lynn,² J. Ma,⁶ Y.G. Ma,²⁹ D. Magestro,²² R. Majka,³⁸ R. Manweiler,³³ S. Margetis,¹⁵ C. Markert,³⁸ L. Martin,³⁰ J. Marx,¹⁶ H.S. Matis,¹⁶ Yu.A. Matulenko,²⁴ T.S. McShane,⁸ F. Meissner,¹⁶ Yu. Melnick,²⁴ A. Meschanin,²⁴ M. Messer,² M.L. Miller,³⁸ Z. Milosevich,⁷ N.G. Minaev,²⁴ C. Mironov,¹⁵ J. Mitchell,²⁶ L. Molnar,²⁵ C.F. Moore,³² M.J. Mora-Corral,¹⁷ V. Morozov,¹⁶ M.M. de Moura,³⁶ M.G. Munhoz,²⁷ J.M. Nelson,³ P. Nevski,² V.A. Nikitin,¹¹ L.V. Nogach,²⁴ B. Norman,¹⁵ S.B. Nurushev,²⁴ G. Odyniec,¹⁶ A. Ogawa,² V. Okorokov,¹⁹ M. Oldenburg,¹⁶ D. Olson,¹⁶ G. Paic,²² S.U. Pandey,³⁶ Y. Panebratsev,¹⁰ S.Y. Panitkin,² A.I. Pavlinov,³⁶ T. Pawlak,³⁴ V. Perevoztchikov,² W. Peryt,³⁴ V.A. Petrov,¹¹ R. Picha,⁵ J. Pluta,³⁴ N. Porile,²⁵ J. Porter,² A.M. Poskanzer,¹⁶ M. Potekhin,² E. Potrebenikova,¹⁰ D. Prindle,³⁵ C. Pruneau,³⁶ J. Putschke,¹⁷ G. Rai,¹⁶ G. Rakness,¹³ O. Ravel,³⁰ R.L. Ray,³² S.V. Razin,^{10,13} D. Reichhold,²⁵ J.G. Reid,³⁵ G. Renault,³⁰ F. Retiere,¹⁶ A. Ridiger,¹⁹ H.G. Ritter,¹⁶ J.B. Roberts,²⁶ O.V. Rogachevski,¹⁰ J.L. Romero,⁵ A. Rose,³⁶ C. Roy,³⁰ L.J. Ruan,^{28,2} V. Rykov,³⁶ I. Sakrejda,¹⁶ S. Salur,³⁸ J. Sandweiss,³⁸ I. Savin,¹¹ J. Schambach,³² R.P. Scharenberg,²⁵ N. Schmitz,¹⁷ L.S. Schroeder,¹⁶ K. Schweda,¹⁶ J. Seger,⁸ D. Seliverstov,¹⁹ P. Seyboth,¹⁷ E. Shahaliev,¹⁰ M. Shao,²⁸ K.E. Shestermanov,²⁴ S.S. Shimanskii,¹⁰ F. Simon,¹⁷ G. Skoro,¹⁰ N. Smirnov,³⁸ R. Snellings,²¹ P. Sorensen,⁶ J. Sowinski,¹³ H.M. Spinka,¹ B. Srivastava,²⁵ S. Stanislaus,³³ E.J. Stephenson,¹³ R. Stock,¹² A. Stolpovsky,³⁶ M. Strikhanov,¹⁹ B. Stringfellow,²⁵ C. Struck,¹² A.A.P. Suaide,³⁶ E. Sugarbaker,²² C. Suire,² M. Šumbera,⁹ B. Surov,² T.J.M. Symons,¹⁶ A. Szanto de Toledo,²⁷ P. Szarwas,³⁴ A. Tai,⁶ J. Takahashi,²⁷ A.H. Tang,^{2,21} P. Sorensen,³⁹ D. Thein,⁶ J.H. Thomas,¹⁶ V. Tikhomirov,¹⁹ M. Tokarev,¹⁰ M.B. Tonjes,¹⁸ T.A. Trainor,³⁵ S. Trentalange,⁶ R.E. Tribble,³¹ V. Trofimov,¹⁹ O. Tsai,⁶ T. Ullrich,² D.G. Underwood,¹ G. Van Buren,² A.M. VanderMolen,¹⁸ A.N. Vasiliev,²⁴ M. Vasiliev,³¹ S.E. Vigdor,¹³ S.A. Voloshin,³⁶ F. Wang,²⁵ G. Wang,¹⁵ X.L. Wang,²⁸ Z.M. Wang,²⁸ H. Ward,³² J.W. Watson,¹⁵ R. Wells,²² G.D. Westfall,¹⁸ C. Whitten Jr.,⁶ H. Wieman,¹⁶ R. Willson,²² S.W. Wissink,¹³ R. Witt,³⁸ J. Wood,⁶ J. Wu,²⁸ N. Xu,¹⁶ Z. Xu,² Z.Z. Xu,²⁸ A.E. Yakutin,²⁴ E. Yamamoto,¹⁶ J. Yang,⁶ P. Yepes,²⁶ V.I. Yurevich,¹⁰ Y.V. Zanevski,¹⁰ I. Zborovský,⁹ H. Zhang,^{38,2} H.Y. Zhang,¹⁵ W.M. Zhang,¹⁵ Z.P. Zhang,²⁸ P.A. Żolnierczuk,¹³ R. Zoukarnееv,¹¹ J. Zoukarnееva,¹¹ and A.N. Zubarev¹⁰

(STAR Collaboration)*

¹Argonne National Laboratory, Argonne, Illinois 60439

²Brookhaven National Laboratory, Upton, New York 11973

³University of Birmingham, Birmingham, United Kingdom

- ⁴University of California, Berkeley, California 94720
⁵University of California, Davis, California 95616
⁶University of California, Los Angeles, California 90095
⁷Carnegie Mellon University, Pittsburgh, Pennsylvania 15213
⁸Creighton University, Omaha, Nebraska 68178
⁹Nuclear Physics Institute AS CR, Řež/Prague, Czech Republic
¹⁰Laboratory for High Energy (JINR), Dubna, Russia
¹¹Particle Physics Laboratory (JINR), Dubna, Russia
¹²University of Frankfurt, Frankfurt, Germany
¹³Indiana University, Bloomington, Indiana 47408
¹⁴Institut de Recherches Subatomiques, Strasbourg, France
¹⁵Kent State University, Kent, Ohio 44242
¹⁶Lawrence Berkeley National Laboratory, Berkeley, California 94720
¹⁷Max-Planck-Institut fuer Physik, Munich, Germany
¹⁸Michigan State University, East Lansing, Michigan 48824
¹⁹Moscow Engineering Physics Institute, Moscow Russia
²⁰City College of New York, New York City, New York 10031
²¹NIKHEF, Amsterdam, The Netherlands
²²Ohio State University, Columbus, Ohio 43210
²³Pennsylvania State University, University Park, Pennsylvania 16802
²⁴Institute of High Energy Physics, Protvino, Russia
²⁵Purdue University, West Lafayette, Indiana 47907
²⁶Rice University, Houston, Texas 77251
²⁷Universidade de Sao Paulo, Sao Paulo, Brazil
²⁸University of Science & Technology of China, Anhui 230027, China
²⁹Shanghai Institute of Nuclear Research, Shanghai 201800, P.R. China
³⁰SUBATECH, Nantes, France
³¹Texas A & M, College Station, Texas 77843
³²University of Texas, Austin, Texas 78712
³³Valparaiso University, Valparaiso, Indiana 46383
³⁴Warsaw University of Technology, Warsaw, Poland
³⁵University of Washington, Seattle, Washington 98195
³⁶Wayne State University, Detroit, Michigan 48201
³⁷Institute of Particle Physics, CCNU (HZNU), Wuhan, 430079 China
³⁸Yale University, New Haven, Connecticut 06520
³⁹University of California, Los Angeles, California 90095
- (Dated: August 26, 2019;)

We report measurements of single-particle inclusive spectra and two-particle azimuthal distributions of charged hadrons at high transverse momentum (high p_T) in minimum bias and central d+Au collisions at $\sqrt{s_{NN}}=200$ GeV. The inclusive yield is enhanced in d+Au collisions relative to binary-scaled p+p collisions, while the two-particle azimuthal distributions are very similar to those observed in p+p collisions. These results demonstrate that the strong suppression of the inclusive yield and back-to-back correlations at high p_T previously observed in central Au+Au collisions are due to final-state interactions with the dense medium generated in such collisions.

PACS numbers: 25.75.-q, 25.75.Dw, 25.75.Gz

Energetic partons propagating through matter are predicted to lose energy through induced gluon radiation, with the magnitude of the energy loss depending strongly on the color charge density [1]. Partonic energy loss is potentially a sensitive probe of the matter created in high energy heavy-ion collisions, where a quark-gluon plasma may form if sufficiently high energy density is achieved. The energetic partons originate in the hard scattering of partons from the incoming nuclei. Direct measurement of jets resulting from parton fragmentation is difficult in nuclear collisions; nevertheless partonic energy loss can be studied using observables such as inclusive spectra and two-particle azimuthal distributions of high trans-

verse momentum (high p_T) hadrons.

Measurements of high p_T hadron production in ultrarelativistic interactions of heavy nuclei reveal strong suppression of both the single-particle inclusive yield [2, 3, 4, 5] and back-to-back pairs (large azimuthal separation $\Delta\phi$) in the most-central, violent collisions, while near-side pairs (small $\Delta\phi$) exhibit jet-like correlations that are similar to those in proton+proton (p+p) collisions [6]. One interpretation of these results is that, in the final state following the hard scattering, energetic partons traversing the dense medium in the core of the collision lose energy, and the observed jets are primarily those created from partons produced near the surface

and directed outwards [6]. Alternatively, the suppression might result from initial-state effects prior to the hard scattering, such as the saturation of gluon densities in the incoming nuclei [7]. Models incorporating either picture are capable of describing central Au+Au collision data [5]. Initial- and final-state effects in Au+Au collisions can be separated through studies of deuteron(d)+Au collisions. Theoretical expectations for d+Au collisions at the Relativistic Heavy Ion Collider (RHIC) are given in [7, 8, 9, 10, 11, 12, 13, 14, 15]. Within a perturbative QCD (pQCD) framework, the expected initial-state nuclear effects in d+Au collisions are multiple scattering prior to a hard collision, which has been used to explain the Cronin enhancement of the inclusive yield [16], and shadowing of the parton distribution functions. Nuclear effects are expected to increase for more central collisions; thus the centrality dependence of observables measured in d+Au collisions also will help reveal their origin.

The STAR Collaboration reports measurements of the inclusive invariant p_T distribution and two-particle azimuthal distributions at high p_T for charged hadrons ($(h^+ + h^-)/2$, approximated by the summed yields of primary π^\pm , K^\pm , p and \bar{p}) in minimum bias and central d+Au collisions at center of mass energy $\sqrt{s_{NN}}=200$ GeV per nucleon pair. Comparison is made to measurements at $\sqrt{s_{NN}}=200$ GeV in the same detector for Au+Au and p+p interactions [5, 6]. The inclusive yield is enhanced in d+Au collisions relative to binary-scaled p+p collisions, in contrast to the large suppression observed in central Au+Au interactions. Similar results are reported in [17, 18]. The d+Au two-particle azimuthal distributions are very similar to those observed in p+p collisions. These observations are consistent with expectations from pQCD models incorporating both the Cronin enhancement and nuclear shadowing [8, 9, 10, 11, 12], and are inconsistent with calculations that attribute the suppression in central Au+Au collisions to initial-state gluon saturation [7].

STAR is a multi-purpose detector [19] located at Brookhaven National Laboratory's RHIC facility. For these measurements, the minimum bias trigger required at least one beam-rapidity neutron in ZDC-Au, the Zero Degree Calorimeter (ZDC) in the Au beam direction, which is assigned negative pseudorapidity (η). This trigger accepts $95\pm 3\%$ of the d+Au hadronic cross section σ_{had}^{dAu} . Trigger backgrounds were measured using beam bunches not in collision. Charged particle momenta were measured by the Time Projection Chamber in a 0.5 T solenoidal magnetic field.

After event selection cuts, the data set consists of 10^7 minimum bias d+Au events. Data were analyzed using the techniques described in [2, 6]. The vertex was reconstructed in $93\pm 1\%$ of triggered minimum bias events. The spectra were corrected for trigger and vertex-finding efficiencies. Contamination of the spectra due to weak decay products was corrected based on HIJING [20]. Re-

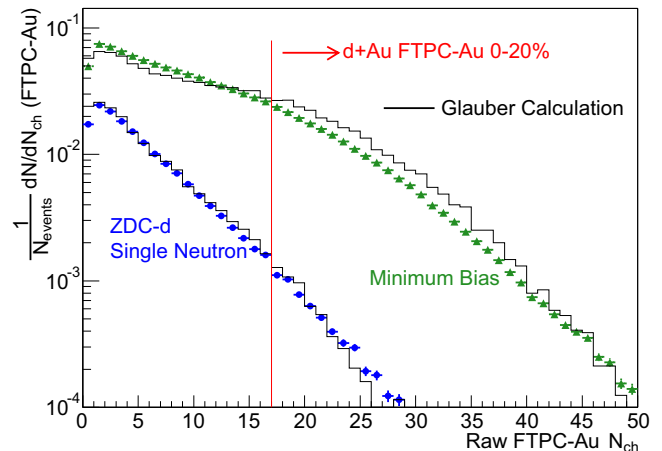


FIG. 1: Uncorrected charged particle multiplicity distributions measured in $-3.8 < \eta < -2.8$ (Au-direction) for d+Au collisions. Points are for minimum bias (triangles) and peripheral (circles, ZDC-d single neutron) collisions. Both are normalized to the total number of d+Au collisions. Histograms are Glauber model calculations.

sults of an independent analysis, using a different technique for vertex reconstruction [5], agree with the reported spectrum within the relative normalization uncertainties at all p_T .

Centrality tagging of d+Au collisions is based on the raw (uncorrected) charged particle multiplicity within $-3.8 < \eta < -2.8$, measured by the Forward Time Projection Chamber in the Au beam direction (FTPC-Au [19]). The FTPC-Au multiplicity was examined in quadrants relative to the orientation of the leading charged hadron at mid-rapidity; auto-correlation effects were found to be negligible. An independent centrality tag, used as a cross-check, requires at least one beam-rapidity (spectator) neutron in ZDC-d, the ZDC in the deuteron beam direction. The cross section for this process in hadronic events was measured to be $(19.2\pm 1.3)\%$ of σ_{had}^{dAu} . ZDC-d and FTPC-Au are separated by 8 rapidity units. Figure 1 shows the FTPC-Au multiplicity for minimum bias and ZDC-d neutron-tagged events. The latter have a strong bias toward low multiplicity.

The centrality tags were modeled using a Monte Carlo Glauber calculation [2] incorporating the Hulthén wavefunction of the deuteron[21]. In this model the mean number of binary collisions $\langle N_{bin} \rangle$ is 7.0 ± 0.3 for minimum bias events and $\sigma_{had}^{dAu}=2.34\pm 0.08$ b. Events with a neutron spectator from the deuteron comprise $(18\pm 3)\%$ of σ_{had}^{dAu} in the model. This event class is biased toward peripheral collisions, with $\langle N_{bin} \rangle=2.7\pm 0.2$. The FTPC-Au multiplicity distribution was modeled by convoluting the Glauber model distribution of participants from the Au nucleus with the charged multiplicity distribution measured in $2.5 < |\eta| < 3.5$ for $\bar{p}+p$ collisions at $\sqrt{s}=200$ GeV[22]. The FTPC-Au acceptance, efficiency and backgrounds were taken into account using HIJING

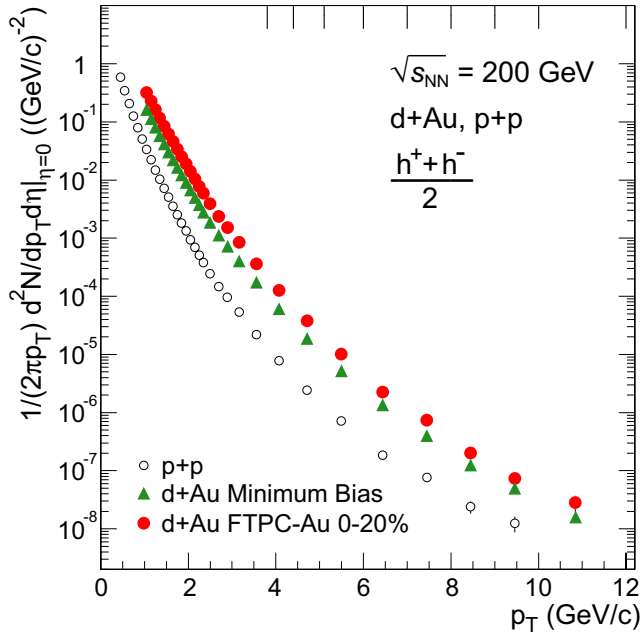


FIG. 2: Inclusive p_T distributions for minimum bias and central d+Au collisions, and non-singly diffractive p+p collisions [5]. Hash marks at the top indicate bin boundaries for $p_T > 3.8$ GeV/c.

[20] events in a GEANT model of the detector. Figure 1 shows the measurements for both minimum bias and ZDC-d neutron-tagged events, together with the corresponding Glauber model predictions. The model is validated by its agreement with both multiplicity distributions and with the ZDC-d single neutron cross section fraction. High FTPC-Au multiplicity therefore biases towards central collisions. Figure 1 shows the cut defining the 20% highest multiplicity collisions in the data. $\langle N_{\text{bin}} \rangle = 12.9 \pm 1.0$ for the 20% highest multiplicity collisions in the Glauber model, where the uncertainty includes the spread in values obtained with several alternative models.

Figure 2 shows the invariant inclusive p_T distribution of $(h^+ + h^-)/2$ within $|\eta| < 0.5$ for minimum bias and central d+Au collisions, together with that for p+p collisions from [5]. The error bars are the quadrature sum of statistical errors and point-to-point systematic uncertainties. The normalization uncertainty for d+Au collisions is 10%.

Nuclear effects on hadron production in d+Au and Au+Au collisions are measured through comparison to the p+p spectrum using the ratio

$$R_{AB}(p_T) = \frac{d^2 N / dp_T d\eta}{T_{AB} d^2 \sigma^{pp} / dp_T d\eta}, \quad (1)$$

where $d^2 N / dp_T d\eta$ is the differential yield per event in the nuclear collision $A + B$, $T_{AB} = \langle N_{\text{bin}} \rangle / \sigma_{\text{inel}}^{pp}$ describes the nuclear geometry, and $d^2 \sigma^{pp} / dp_T d\eta$ for p+p inelastic collisions is determined from the measured p+p differential

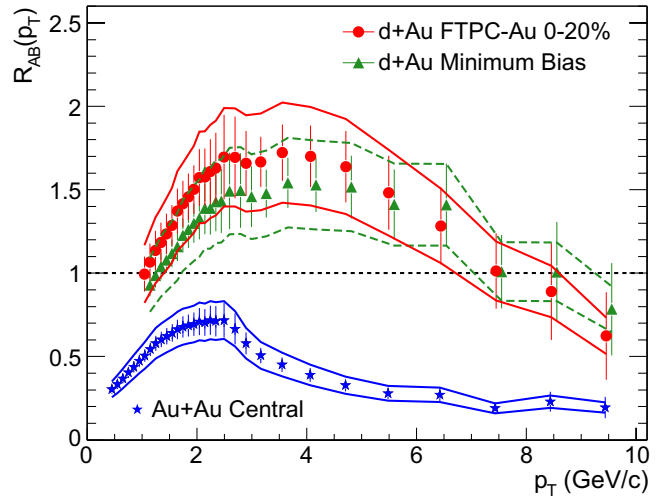


FIG. 3: $R_{AB}(p_T)$ from Eq. 1 for minimum bias and central d+Au collisions, and central Au+Au collisions[5]. The minimum bias d+Au data are displaced 100 MeV/c to the right for clarity. The bands show the normalization uncertainties, which are highly correlated point-to-point and between the two d+Au distributions.

cross section[5]. In the absence of nuclear effects such as shadowing, the Cronin effect, or gluon saturation, hard processes are expected to scale with the number of binary collisions and $R_{AB}(p_T) = 1$. Figure 3 shows $R_{AB}(p_T)$ for minimum bias and central d+Au collisions. The error bars are the quadrature sum of the statistical and point-to-point systematic uncertainties. $R_{AB}(p_T) > 1$ for $2 < p_T < 7$ GeV/c. $R_{AB}(p_T)$ for central and minimum bias d+Au collisions contain many common uncertainties, including dependence on the same p+p reference spectrum. The ratio of $R_{AB}(p_T)$ for central relative to minimum bias collisions, which factors out these common uncertainties, is 1.11 ± 0.03 at 4 GeV/c, consistent with expectations from the Cronin effect [12]. In addition $R_{AB}(p_T)$ may be influenced by nuclear shadowing [13] and its centrality dependence [14]. Figure 3 also shows $R_{AB}(p_T)$ for central Au+Au collisions[5], exhibiting large suppression in hadron production at high p_T .

Figure 4(a) shows the two-particle azimuthal distribution $D(\Delta\phi)$, defined as

$$D(\Delta\phi) \equiv \frac{1}{N_{\text{trigger}}} \frac{1}{\epsilon} \frac{dN}{d(\Delta\phi)}, \quad (2)$$

for minimum bias and central d+Au collisions, and for p+p collisions[6]. Only particles within $|\eta| < 0.7$ are included in the analysis. N_{trigger} is the number of particles within $4 < p_T(\text{trig}) < 6$ GeV/c, referred to as trigger particles. The distribution results from the correlation of each trigger particle with all associated particles in the same event having $2 < p_T < p_T(\text{trig})$, where ϵ is the tracking efficiency of the associated particles. The normalization uncertainties are less than 5%.

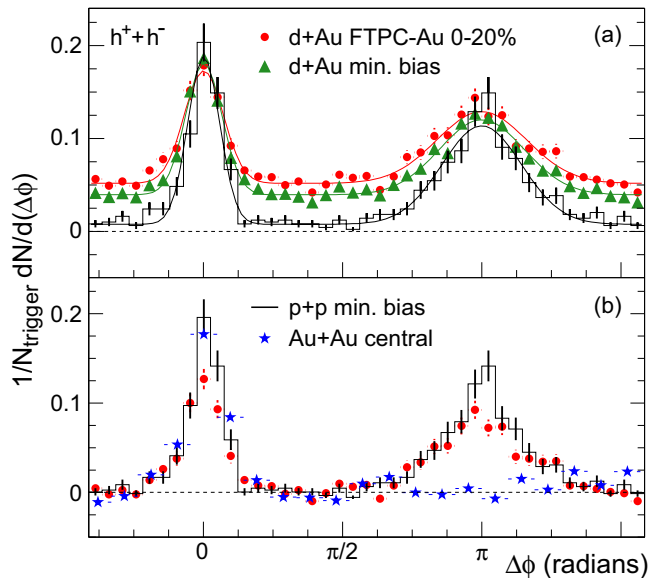


FIG. 4: (a) Efficiency corrected two-particle azimuthal distributions for minimum bias and central d+Au collisions, and for p+p collisions [6]. Curves are fits using Eq. 3, with parameters given in Table I. (b) Comparison of two-particle azimuthal distributions for central d+Au collisions to those seen in p+p and central Au+Au collisions [6]. The respective pedestals have been subtracted.

TABLE I: Fit parameters from Eq. 3. Errors are statistical only.

	p+p min. bias	d+Au min. bias	d+Au central
A_N	0.081 ± 0.005	0.073 ± 0.003	0.067 ± 0.004
σ_N	0.18 ± 0.01	0.20 ± 0.01	0.22 ± 0.02
A_B	0.119 ± 0.007	0.097 ± 0.004	0.098 ± 0.007
σ_B	0.45 ± 0.03	0.48 ± 0.02	0.51 ± 0.03
P	0.008 ± 0.001	0.039 ± 0.001	0.052 ± 0.002

The azimuthal distributions in d+Au collisions include a near-side ($\Delta\phi \sim 0$) peak similar to that seen in p+p and Au+Au collisions [6] that is typical of jet production, and a back-to-back ($\Delta\phi \sim \pi$) peak similar to that seen in p+p and peripheral Au+Au collisions [6] that is typical of di-jet events. The azimuthal distributions are characterized by a fit to the sum of near-side (first term) and back-to-back (second term) Gaussian peaks and a constant:

$$D(\Delta\phi) = A_N \frac{e^{-(\Delta\phi)^2/2\sigma_N^2}}{\sqrt{2\pi}\sigma_N} + A_B \frac{e^{-(|\Delta\phi|-\pi)^2/2\sigma_B^2}}{\sqrt{2\pi}\sigma_B} + P. \quad (3)$$

Fit parameters are given in Table I. Their systematic uncertainties are highly correlated between the data sets, and are less than 20% for σ_N and less than 10% for all other parameters. The only large difference in the azimuthal distributions in p+p and d+Au collisions is the growth of the pedestal P . It increases with increasing $\langle N_{\text{bin}} \rangle$, but is not proportional to $\langle N_{\text{bin}} \rangle$ as might be ex-

pected for incoherent production. Both σ_N and σ_B exhibit at most a small increase from p+p to central d+Au collisions. A small growth in σ_B is expected to result from initial-state multiple scattering [23, 24]. The modest reduction in the correlation strengths A_N and A_B from p+p to central d+Au collisions is similar to that seen previously for peripheral Au+Au collisions [6].

Figure 4(b) shows the pedestal-subtracted azimuthal distributions for p+p and central d+Au collisions. The azimuthal distributions are shown also for central Au+Au collisions after subtraction of the elliptic flow and pedestal contributions [6]. The near-side peak is similar in all three systems, while the back-to-back peak in central Au+Au shows a dramatic suppression relative to p+p and d+Au.

The contrast between d+Au and central Au+Au collisions in Figs. 3 and 4 indicates that the cause of the strong high p_T suppression observed previously is associated with the medium produced in Au+Au but not in d+Au collisions. The suppression of the inclusive hadron yield at high p_T in central Au+Au collisions has been discussed theoretically in various approaches (see [5] for references). Measurements of central Au+Au collisions [5] are described both by pQCD calculations that incorporate shadowing, the Cronin effect, and partonic energy loss in dense matter, and by a calculation extending the saturation model to high momentum transfer. However, predictions of these models differ significantly for d+Au collisions. Due to the Cronin effect, pQCD models predict that $R_{AB}(p_T) > 1$ within $2 < p_T < 6$ GeV/c for minimum bias d+Au collisions, with a peak magnitude of 1.1-1.5 in the range $2.5 < p_T < 4$ GeV/c [11]. The enhancement is expected to be larger for central collisions [12]. The saturation model calculation in [7] predicts $R_{AB}(p_T) < 1$, with larger suppression for more central events, achieving $R_{AB}(p_T) \sim 0.75$ for the 20% most central collisions. In contrast, another saturation model calculation [15] generates an enhancement in $R_{AB}(p_T)$, similar to the Cronin effect, for both d+Au and Au+Au collisions. Figure 3 shows that $R_{AB}(p_T)$ is qualitatively different in d+Au and central Au+Au collisions: in d+Au, $R_{AB}(p_T)$ significantly exceeds unity and is larger for central than for minimum bias collisions. These results are consistent with expectations from pQCD calculations but not the saturation model in [7]. Scattering of the hadronic fragments of jets also may contribute to the suppression of the inclusive yield [5, 25].

The azimuthal distributions of back-to-back jets and high p_T di-hadrons have been observed to broaden in fixed-target p+nucleus collisions relative to p+p collisions, but are not strongly suppressed [23]. Slight broadening of the back-to-back hadron distribution in d+Au collisions at $\sqrt{s_{NN}} = 200$ GeV is also expected from pQCD models incorporating the Cronin effect [24]. Predictions of the saturation model for the back-to-back hadron distributions require further theoretical develop-

ment, though the rate may be suppressed due to a mono-jet contribution [26]. Table I shows that the distribution of back-to-back high p_T hadrons is not substantially modified in central d+Au collisions relative to p+p collisions, consistent with expectations from pQCD calculations.

In summary, we have reported the inclusive p_T distributions and two-particle azimuthal distributions of high p_T hadrons in minimum bias and central d+Au collisions at $\sqrt{s_{NN}}=200$ GeV. Similar measurements for Au+Au and p+p interactions have revealed a striking suppression of both the inclusive hadron yield and the back-to-back correlations for central Au+Au collisions. If the suppression is the result of initial-state effects, it also should be observed in d+Au collisions. No suppression in d+Au collisions is observed. Rather, the inclusive yield is enhanced and the two-particle azimuthal distributions exhibit little change relative to p+p. These results suggest that the Cronin effect plays a significant role in d+Au collisions for $2 < p_T < 7$ GeV/c. We conclude that the suppression phenomena seen in central Au+Au collisions are due to final-state interactions with the dense system generated in the collision.

We wish to thank the RHIC Operations Group and the RHIC Computing Facility at Brookhaven National Laboratory, and the National Energy Research Scientific Computing Center at Lawrence Berkeley National Laboratory for their support. This work was supported by the Division of Nuclear Physics and the Division of High Energy Physics of the Office of Science of the U.S. Department of Energy, the United States National Science Foundation, the Bundesministerium fuer Bildung und Forschung of Germany, the Institut National de la Physique Nucleaire et de la Physique des Particules of France, the United Kingdom Engineering and Physical Sciences Research Council, Fundacao de Amparo a Pesquisa do Estado de Sao Paulo, Brazil, the Russian Ministry of Science and Technology, the Ministry of Education of China, the National Natural Science Foundation of China, Stichting voor Fundamenteel Onderzoek der Materie, the Grant Agency of the Czech Republic and the Swiss National Science Foundation.

- [1] R. Baier, D. Schiff and B. G. Zakharov, *Ann. Rev. Nucl. Part. Sci.* **50**, 37 (2000); M. Gyulassy, I. Vitev, X.N. Wang, B. Zhang, nucl-th/0302077.
- [2] C. Adler *et al.*, *Phys. Rev. Lett.* **89**, 202301 (2002); B. Choi, Ph.D. Dissertation, University of Texas (2003).
- [3] K. Adcox *et al.*, *Phys. Rev. Lett.* **88**, 022301 (2002); *Phys. Lett.* **B561**, 82 (2003); S.S. Adler *et al.*, nucl-ex/0304022.
- [4] B.B. Back *et al.*, nucl-ex/0302015.
- [5] J. Adams *et al.*, nucl-ex/0305015.
- [6] C. Adler *et al.*, *Phys. Rev. Lett.* **90**, 082302 (2003).
- [7] D. Kharzeev, E. Levin, and L. McLerran, *Phys. Lett.* **561**, 93 (2003).
- [8] X.N. Wang, *Phys. Rev.* **C61**, 064910 (2000); nucl-th/0303004.
- [9] Y. Zhang *et al.*, *Phys. Rev.* **C65**, 034903 (2002).
- [10] B.Z. Kopeliovich *et al.*, *Phys. Rev. Lett.* **88**, 232303 (2002).
- [11] A. Accardi, hep-ph/0212148, and references therein.
- [12] I. Vitev, *Phys. Lett.* **B562**, 36 (2003).
- [13] K.J. Eskola and H. Honkanen, *Nucl. Phys.* **A713**, 167 (2003).
- [14] S.R. Klein and R. Vogt, nucl-th/0305046.
- [15] R. Baier, A. Kovner and U. Wiedemann, hep-ph/0305265.
- [16] D. Antreaysan *et al.*, *Phys. Rev.* **D19**, 764 (1979).
- [17] S.S. Adler *et al.*, nucl-ex/0306021.
- [18] B.B. Back *et al.*, nucl-ex/0306025.
- [19] K.H. Ackermann *et al.*, *Nucl. Instr. Meth.* **A499**, 624 (2003).
- [20] X.N. Wang and M. Gyulassy, *Phys. Rev.* **D44**, 3501 (1991). Version 1.382 is used.
- [21] D. Kharzeev, E. Levin and M. Nardi, hep-ph/0212316; L. Hulthén and M. Sagawara, *Handbuch der Physik* **39** (1957).
- [22] R.E. Ansorge *et al.*, *Z. Phys.* **C43**, 357 (1989).
- [23] M.D. Corcoran *et al.*, *Phys. Lett* **B259**, 209 (1991); T. Fields and M.D. Corcoran, *Phys. Rev. Lett.* **70**, 143 (1993).
- [24] J. Qiu and I. Vitev, nucl-th/0306039.
- [25] K. Gallmeister, C. Greiner and Z. Xu, *Phys. Rev.* **C67**, 044905 (2003).
- [26] D. Kharzeev, *Nucl. Phys.* **A715**, 35c (2003).

* URL: www.star.bnl.gov